Computed tomography (CT)

Part 2

J. Kybic and André Sopczak[1]

2005–2024

[1] Using images from J. Hozman, J. Fessler, S. Webb, M. Slaney, A. Kak and others

Reconstruction methods

- *Backprojection* (not an inverse)
- *Fourier reconstruction* (slow)
- Filtered backprojection
- Algebraic reconstruction (iterative)

Forward projection

sinogram

$$P_\varphi(r) = \int_{(x,y)\in L(r,\varphi)} \mu(x,y)\mathrm{d}l$$

$$r = x\cos\varphi + y\sin\varphi$$

$$P_\varphi(r) = \int_t \mu(x,y)\mathrm{d}t$$

$$x = r\cos\varphi - t\sin\varphi$$

$$y = r\sin\varphi + t\cos\varphi$$

Variable correspondence:

$$\xi' = r, \quad \eta' = t, \quad \xi = x, \quad \eta = y$$

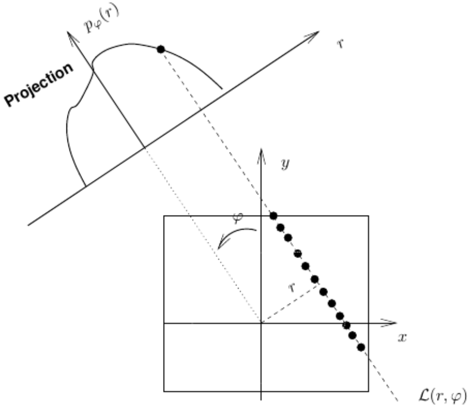

Backprojection

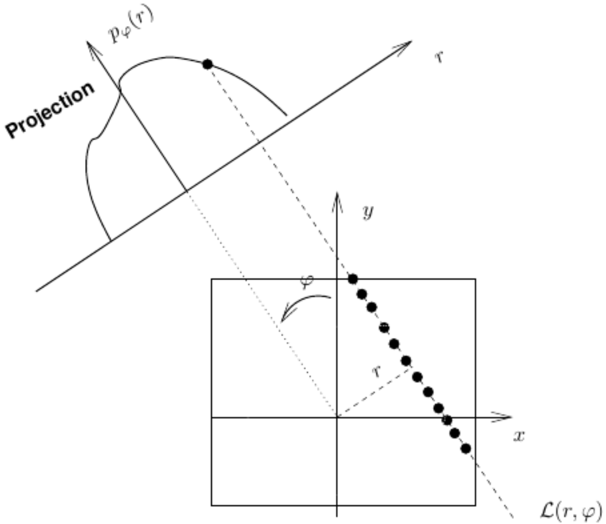

Backprojection

$$\mu_b(x,y) = \int_0^{\pi} P_\varphi(r)\,\mathrm{d}\varphi$$

$$r = x\cos\varphi + y\sin\varphi$$

for uniformly discretized φ

$$\varphi_i = \pi(i-1)/n_\varphi, \quad i = 1,\ldots,n_\varphi$$

$$\mu_b(x,y) \approx \frac{\pi}{n_\varphi}\sum_{i=1}^{n_\varphi} P_\varphi(x\cos\varphi_i + y\sin\varphi_i)$$

Backprojection

. . . is **not** an inverse of the Radon transform, leads to *star artifacts*

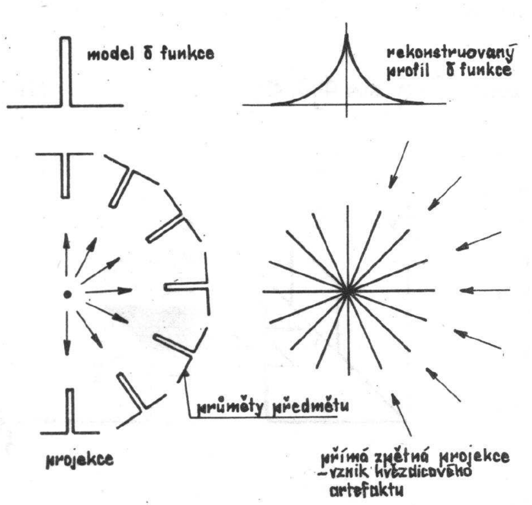

Backprojection

. . . is **not** an inverse of the Radon transform, leads to *star artifacts*

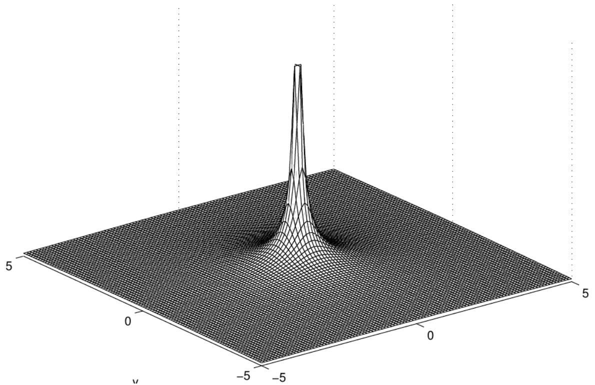

Backprojection

...is **not** an inverse of the Radon transform, leads to *star artifacts*

laminogram μ_b — the original object μ blurred, convolved by $1/|r|$

Central slice theorem

(Projection Theorem, Věta o centrálním řezu)

$$P_\varphi(r) = \int \mu(r\cos\varphi - t\sin\varphi, r\sin\varphi + t\cos\varphi)\mathrm{d}t$$

Fourier transform of the Radon transform by r:

$$\begin{aligned}\mathscr{F}\{\mathscr{R}[\mu(x,y)]\} = \mathscr{F}\{P_\varphi(r)\} = \hat{P}_\varphi(\omega) &= \int P_\varphi(r)\mathrm{e}^{-2\pi j\omega r}\mathrm{d}r \\ &= \iint \mu(r\cos\varphi - t\sin\varphi, r\sin\varphi + t\cos\varphi)\mathrm{e}^{-2\pi j\omega r}\mathrm{d}r\mathrm{d}t\end{aligned}$$

Substitution $(r,t) \to (x,y)$:

$$\hat{P}_\varphi(\omega) = \iint \mu(x,y)\mathrm{e}^{-2\pi j\omega(x\cos\varphi + y\sin\varphi)}\mathrm{d}x\mathrm{d}y$$

Central slice theorem

$$\hat{P}_\varphi(\omega) = \iint \mu(x,y)\mathrm{e}^{-2\pi j\omega(x\cos\varphi + y\sin\varphi)}\mathrm{d}x\mathrm{d}y$$

Denote $u = \omega\cos\varphi \quad v = \omega\sin\varphi$

$$\hat{P}(u,v) = \iint \mu(x,y)\mathrm{e}^{-2\pi j(xu+yv)}\mathrm{d}x\mathrm{d}y$$

and therefore

$$\begin{aligned}\hat{P}(u,v) &= \mathscr{F}\{\mu(x,y)\}\\ \hat{P}_\varphi(\omega) &= \mathscr{F}\{\mu(x,y)\}(\omega\cos\varphi, \omega\sin\varphi) = \hat{\mu}(\omega\cos\varphi, \omega\sin\varphi)\end{aligned}$$

Central slice theorem

$$\hat{P}(u,v) = \mathscr{F}\{\mu(x,y)\}$$
$$\hat{P}_\varphi(\omega) = \mathscr{F}\{\mu(x,y)\}(\omega\cos\varphi, \omega\sin\varphi) = \hat{\mu}(\omega\cos\varphi, \omega\sin\varphi)$$

Slice of the 2D Fourier transform of the image μ at angle φ is the 1D Fourier transform of the projection P_φ of the same image μ.

Fourier reconstruction

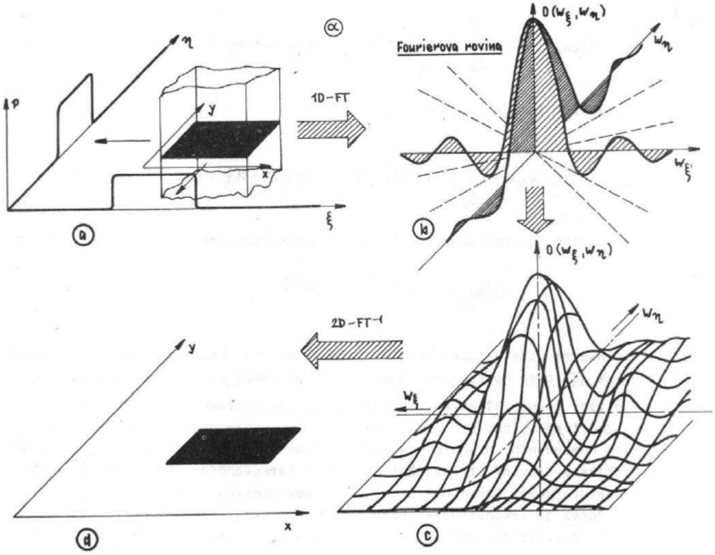

Fourier reconstruction (2)

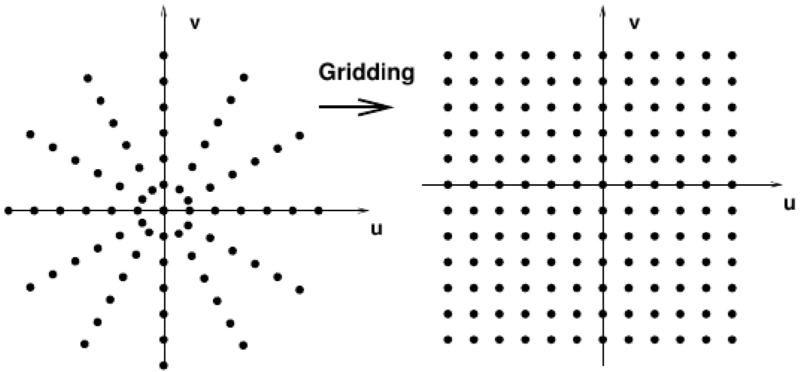

- 1D FT $\hat{P}_\varphi(\omega)$ of each projection $P_\varphi(r)$
- Interpolate FT from polar to Cartesian grid (to get $\hat{P}(u, v)$)
- Inverse 2D FT $\hat{P}(u, v)$ to get object μ

Cons: computational complexity, interpolation artifacts

Inverse Radon transform

From the Fourier slice theorem:

$$\hat{P}(u,v) = \mathscr{F}\left\{\mu(x,y)\right\}$$

$$\mu(x,y) = \mathscr{F}^{-1}\left\{\hat{P}(u,v)\right\} = \int_{-\infty}^{\infty}\int_{-\infty}^{\infty} \hat{P}(u,v)\mathrm{e}^{2\pi j(xu+yv)}\mathrm{d}u\mathrm{d}v$$

Polar coordinates $u = \omega\cos\varphi, \quad v = \omega\sin\varphi$:

$$\mu(x,y) = \int_{0}^{\pi}\int_{-\infty}^{\infty} \hat{P}_{\varphi}(\omega)\mathrm{e}^{2\pi j\omega(x\cos\varphi+y\sin\varphi)}|\omega|\mathrm{d}\omega\mathrm{d}\varphi$$

where $|\omega|$ is the Jacobian (determinant) of $(\omega,\phi)\to(u,v)$

$$\begin{vmatrix} \frac{\partial u}{\partial\varphi} & \frac{\partial u}{\partial\omega} \\ \frac{\partial v}{\partial\varphi} & \frac{\partial v}{\partial\omega} \end{vmatrix} = \left|-\omega\sin^2\varphi - \omega\cos^2\varphi\right| = |\omega|$$

Inverse Radon transform

$$\mu(x, y) = \int_0^\pi \int_{-\infty}^\infty \hat{P}_\varphi(\omega) \mathrm{e}^{2\pi j\omega(x\cos\varphi + y\sin\varphi)} |\omega| \mathrm{d}\omega \mathrm{d}\varphi$$

can be written as

$$\mu(x, y) = \int_0^\pi Q_\varphi(\underbrace{x\cos\varphi + y\sin\varphi}_{r}) \mathrm{d}\varphi$$

$$Q_\varphi(r) = \int_{-\infty}^\infty \hat{P}_\varphi(\omega) \mathrm{e}^{2\pi j\omega r} |\omega| \mathrm{d}\omega$$

where $Q_\varphi(r)$ is a modified projection

Inverse Radon transform

$$\mu(x,y) = \int_0^\pi Q_\varphi(r)\mathrm{d}\varphi$$

$$Q_\varphi(r) = \int_{-\infty}^{\infty} \hat{P}_\varphi(\omega)\mathrm{e}^{2\pi j\omega r}|\omega|\mathrm{d}\omega$$

$$Q_\varphi(r) = \mathscr{F}^{-1}\left\{|\omega|\hat{P}_\varphi(\omega)\right\} = \mathscr{F}^{-1}\left\{|\omega|\right\} * P_\varphi(r)$$

defining the exact inverse Radon transform

$$P_\varphi(r) = \mathscr{R}\left[\mu(x,y)\right]$$

$$\mu(x,y) = \mathscr{R}^{-1}\left[P_\varphi(r)\right]$$

Filtered backprojection

Filtrovaná zpětná projekce

- Filter all projections $P_\varphi(r)$ for all φ, get modified projections $Q_\varphi(r)$
- Backproject modified projections and sum

$$\mu(x, y) = \int_0^\pi Q_\varphi(r) \mathrm{d}\varphi$$

$$Q_\varphi(r) = h(t) * P_\varphi(r) = \mathscr{F}^{-1}\{H(\omega)\} * P_\varphi(r)$$

$$H(\omega) = |\omega|$$

- No Fourier transform involved.

Practical implementation of filtered backprojection

- **Problem:** Ideal filter $H(\omega) = |\omega|$ amplifies noise
- **Solution:** Make $\hat{P}_\varphi(\omega)$ frequency limited. Ramakrishnan-Lakshiminaryanan $\longrightarrow$ Ram-Lak filter:

$$H(\omega) = \begin{cases} |\omega| & \text{if } |\omega| \leq \Omega \\ 0 & \textit{otherwise} \end{cases}$$

Practical implementation of filtered backprojection

- **Problem:** Ideal filter $H(\omega) = |\omega|$ amplifies noise
- **Solution:** Make $\hat{P}_\varphi(\omega)$ frequency limited. Ramakrishnan-Lakshiminaryanan $\longrightarrow$ Ram-Lak filter:

$$H(\omega) = \begin{cases} |\omega| & \text{if } |\omega| \leq \Omega \\ 0 & \textit{otherwise} \end{cases}$$

- Ram-Lak filter causes artefacts (Gibbs). Many solutions (Hamming filter, Shepp-Logan filter). Tradeoff between SNR and resolution.

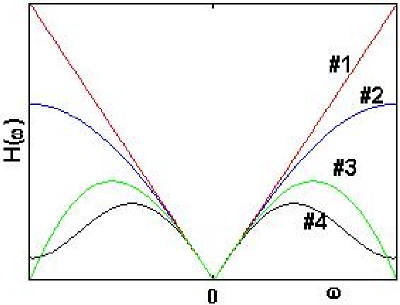

Bandlimited ramp filter *h*

in space domain

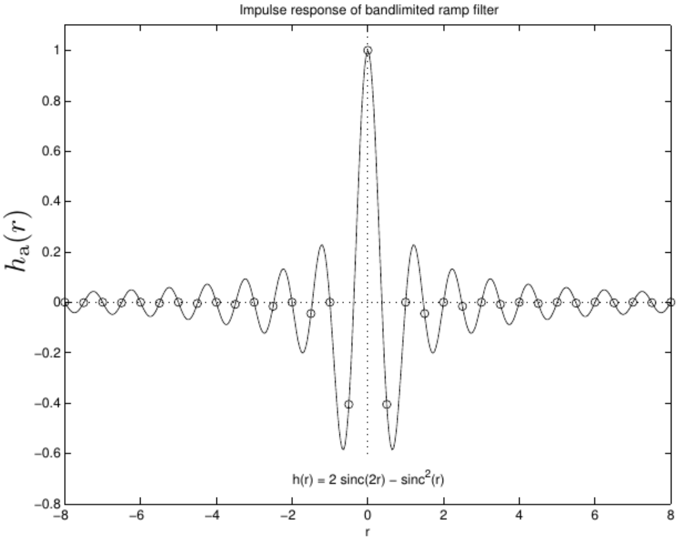

Filtered backprojection example

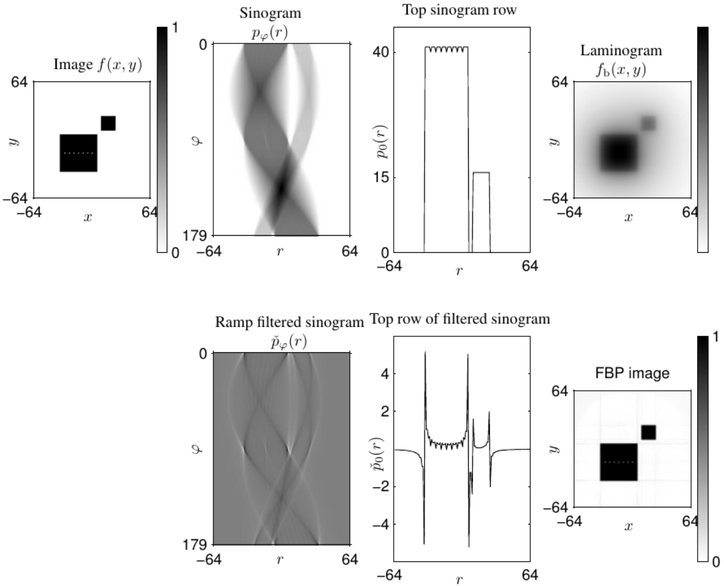

Filtered backprojection

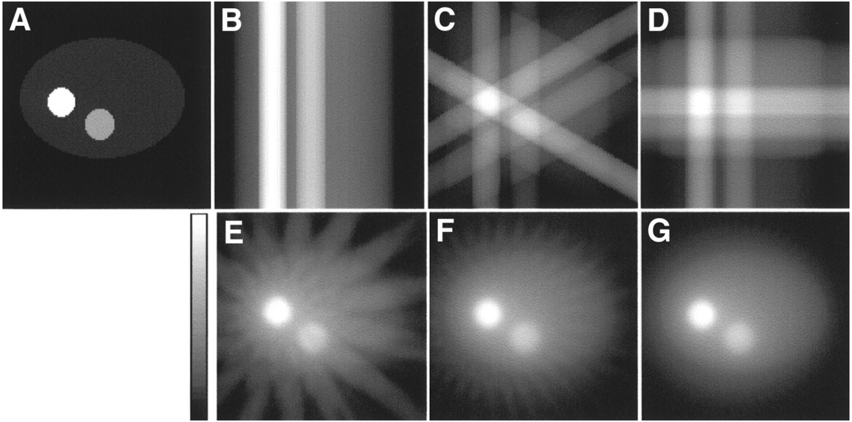

original image, 1,3, 4, 16, 32, a 64 projections

Fan-beam reconstruction

- Rays not parallel, not a Radon transform.

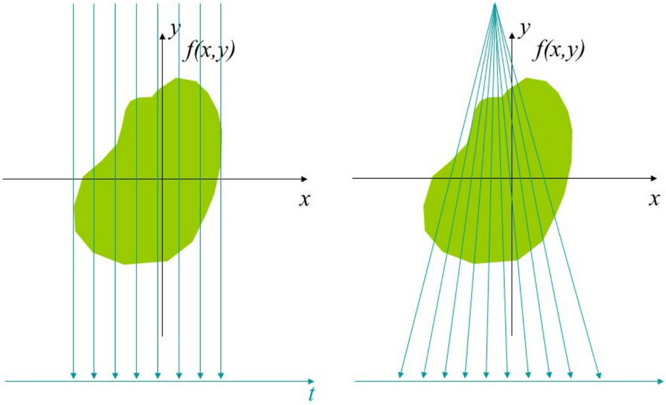

image courtesy of Gillian Henderson

Fan-beam reconstruction

- Rays not parallel, not a Radon transform.
- Rebinning

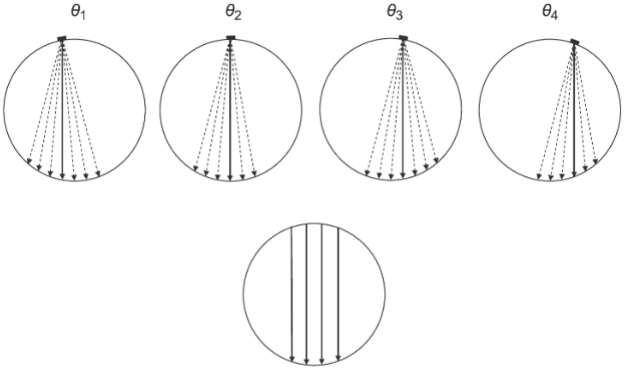

image courtesy of Jonathan Mamou and Yao Wang

Fan-beam reconstruction (2)

- Rays not parallel, not a Radon transform.
- Exact algorithms:
  - Rebinning
  - filtered backprojection (Katsevich) — computational complexity, increased dose.
- Approximate algorithms: Modified filtered backprojection (quadratic cosine correction, $\cos\theta$). Feldkamp-Davis-Kress

Fan-beam reconstruction (2)

- Rays not parallel, not a Radon transform.
- Exact algorithms:
  - Rebinning
  - filtered backprojection (Katsevich) — computational complexity, increased dose.
- Approximate algorithms: Modified filtered backprojection (quadratic cosine correction, $\cos\theta$). Feldkamp-Davis-Kress
- Algebraic reconstruction. Best quality but slow.

Analytical methods

Algebraic reconstruction

3D CT

Radiation dose

Algebraic reconstruction

- Setup and solve a (large) system of equations describing the measurements.
- Mostly (but not necessarily) linear

Algebraic reconstruction

- Setup and solve a (large) system of equations describing the measurements.
- Mostly (but not necessarily) linear

Advantages over FBP

- Better modeling of the physics — attenuation, scattering, limited resolution, beam geometry, sensor noise, beam hardening...
- Flexible, better handling of limited acquisition — restricted region, restricted angles, few measurements required
- Can use a statistical image model (regularization)
- Higher quality, less apparent artifacts

Disadvantage — speed

FBP versus ART

few projections

Phantom

FBP `(iradon)`

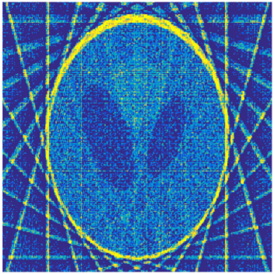

ART w/ box constraints

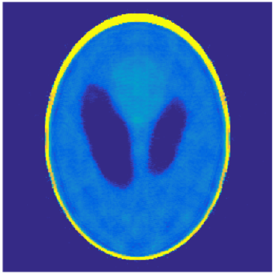

Courtesy of Technical University of Denmark

FBP versus ART

missing angles

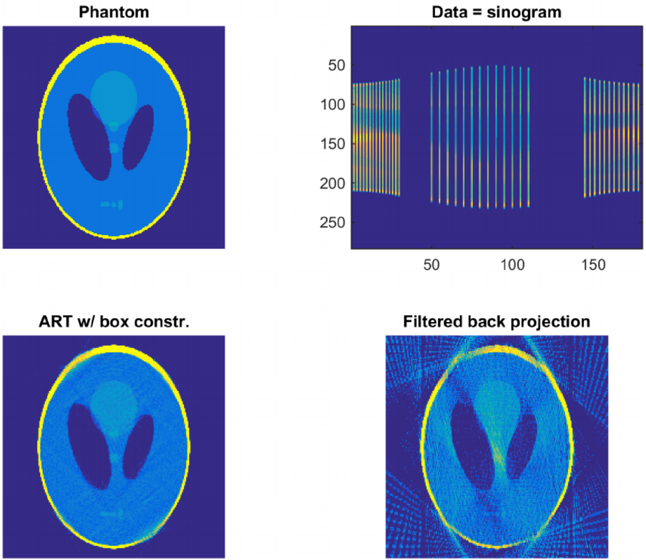

Courtesy of Technical University of Denmark

Linear reconstruction

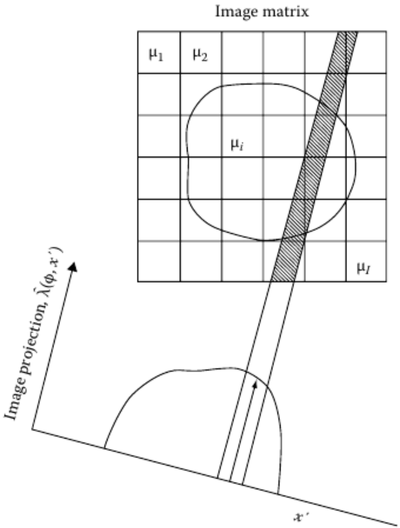

Linear reconstruction

- Discretize continuous $\mu(\mathbf{x})$ to pixels μ_i

$$\mu(\mathbf{x}) = \sum_{i=1}^{M} \mu_i \psi_i(\mathbf{x})$$

- Basis functions (piecewise constant, P0)

$$\psi_i(\mathbf{x}) = \begin{cases} 1, \text{if } \mathbf{x} \text{ in pixel } i \\ 0, \text{otherwise} \end{cases}$$

Linear reconstruction

- Discretize continuous $\mu(\mathbf{x})$ to pixels μ_i

$$\mu(\mathbf{x}) = \sum_{i=1}^{M} \mu_i \psi_i(\mathbf{x})$$

- Basis functions (piecewise constant, P0)

$$\psi_i(\mathbf{x}) = \begin{cases} 1, \text{if } \mathbf{x} \text{ in pixel } i \\ 0, \text{otherwise} \end{cases}$$

- Radon transform

$$P_\varphi(r) = \mathscr{R}[\mu](\varphi, r) = \sum_{i=1}^{M} \mu_i \mathscr{R}[\psi_i](\varphi, r)$$

Linear reconstruction (2)

- For all projections $p_j = P_{\varphi_j}(r_j)$, $j = 1, \ldots, N$

$$p_j = P_{\varphi_j}(r_j) = \sum_{i=1}^{M} \mu_i \underbrace{\mathscr{R}[\psi_i](\varphi_j, r_j)}_{w_{ij}}$$

$$p_j = \sum_{i=1}^{M} w_{ij} \mu_i$$

$$\mathbf{p} = \mathrm{W} \boldsymbol{\mu}$$

where μ_i are pixel values, p_j are the projections.

Knowing $\mathbf{p}$, solve for $\boldsymbol{\mu}$.

Linear reconstruction (2)

- For all projections $p_j = P_{\varphi_j}(r_j)$, $j = 1, \ldots, N$

$$p_j = P_{\varphi_j}(r_j) = \sum_{i=1}^{M} \mu_i \underbrace{\mathscr{R}[\psi_i](\varphi_j, r_j)}_{w_{ij}}$$

$$p_j = \sum_{i=1}^{M} w_{ij} \mu_i$$

$$\mathbf{p} = \mathrm{W} \boldsymbol{\mu}$$

  where μ_i are pixel values, p_j are the projections.

  Knowing $\mathbf{p}$, solve for $\boldsymbol{\mu}$.

- Linear equation system
  - is big ($10^4 \sim 10^6$ unknowns and measurements)
  - can be overdetermined
  - can be underdetermined
  - is sparse

Weight coefficients

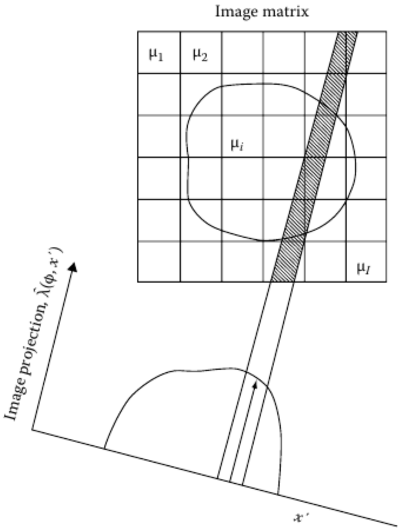

Weight coefficients

For line rays — intersection length

$$w_{ij} = \int\limits_{\mathbf{x} \in L(r_j, \varphi_j)} \psi_i(\mathbf{x}) \mathrm{d}l$$

For thick rays — intersection area

$$w_{ij} = \int\limits_{\mathbf{x} \in L'(r_j, \varphi_j)} \psi_i(\mathbf{x}) \mathrm{d}\mathbf{x}$$

Weight coefficients

For line rays — intersection length

$$w_{ij} = \int_{\mathbf{x} \in L(r_j, \varphi_j)} \psi_i(\mathbf{x}) \mathrm{d}l$$

Binary approximation

$$w_{ij} = \begin{cases} 1, & \text{if ray } L(r_j, \varphi_j) \text{ intersects pixel } \psi_i \\ 0, & \text{otherwise} \end{cases}$$

Least squares solution

for overdetermined systems

Minimize the reconstruction error $\mathbf{e}$

$$\boldsymbol{\mu}^* = \arg\min_{\boldsymbol{\mu}} \|\underbrace{\mathrm{W}\boldsymbol{\mu} - \mathbf{p}}_{\mathbf{e}}\|^2$$

Least squares solution

for overdetermined systems

Minimize the reconstruction error **e**

$$\boldsymbol{\mu}^* = \arg\min_{\boldsymbol{\mu}} \|\underbrace{\mathrm{W}\boldsymbol{\mu} - \mathbf{p}}_{\mathbf{e}}\|^2$$

The reconstruction error **e** must be perpendicular to *range* of W.

$$0 = \mathrm{W}^T\mathbf{e} = \mathrm{W}^T(\mathrm{W}\boldsymbol{\mu}^* - \mathbf{p})$$

Normal equations

$$\mathrm{W}^T\mathbf{p} = \mathrm{W}^T\mathrm{W}\boldsymbol{\mu}^*$$

Pseudoinverse solution

$$\boldsymbol{\mu}^* = (\mathrm{W}^T\mathrm{W})^{-1}\mathrm{W}^T\mathbf{p}$$

suitable for smaller problems

Minimum-norm solution

for underdetermined systems or noisy data

Add regularization D

$$\boldsymbol{\mu}^* = \arg\min_{\boldsymbol{\mu}} \|\underbrace{\mathrm{W}\boldsymbol{\mu} - \mathbf{p}}_{\mathbf{e}}\|^2 + \lambda\|\mathrm{D}\boldsymbol{\mu}\|^2$$

Normal equations

$$\mathrm{W}^T\mathbf{p} = (\mathrm{W}^T\mathrm{W} + \lambda\mathrm{D}^T\mathrm{D})\boldsymbol{\mu}^*$$

Pseudoinverse solution

$$\boldsymbol{\mu}^* = (\mathrm{W}^T\mathrm{W} + \lambda\mathrm{D}^T\mathrm{D})^{-1}\mathrm{W}^T\mathbf{p}$$

Iterative methods

Principles

- Start from an initial guess of $\boldsymbol{\mu}$
- Compare measured projections and simulations
- Correct pixel values to decrease the difference
- Iterate until convergence

Properties

- Take advantage of the sparseness (complexity $O(N)$ per iteration)
- Low memory complexity ($O(M)$)
- $\longrightarrow$ Suitable for large systems of equations
- Early stopping
- Slower for small problems (compared to direct methods)

Projection method

Kaczmarz's method

$$p_j = \sum_{i=1}^{M} w_{ij}\mu_i, \qquad j = 1, 2, \ldots, N$$

$$p_j = \langle \mathbf{w}_j, \boldsymbol{\mu} \rangle = \mathbf{w}_j^T \boldsymbol{\mu}$$

Projection method

Kaczmarz's method

$$p_j = \sum_{i=1}^{M} w_{ij}\mu_i, \qquad j = 1, 2, \ldots, N$$

$$p_j = \langle \mathbf{w}_j, \boldsymbol{\mu} \rangle = \mathbf{w}_j^T \boldsymbol{\mu}$$

- Affine solution space of equation j

$$\mathcal{S}_j = \{\boldsymbol{\mu} \in \mathbb{R}^M; p_j = \langle \mathbf{w}_j, \boldsymbol{\mu} \rangle\}$$

Normal vector $\mathbf{w}_j$

$$\forall \boldsymbol{\mu} \in \mathcal{S}_j, \boldsymbol{\mu}' \in \mathcal{S}_j;\ \langle \mathbf{w}_j, \boldsymbol{\mu} - \boldsymbol{\mu}' \rangle = 0$$

Projection to an affine space

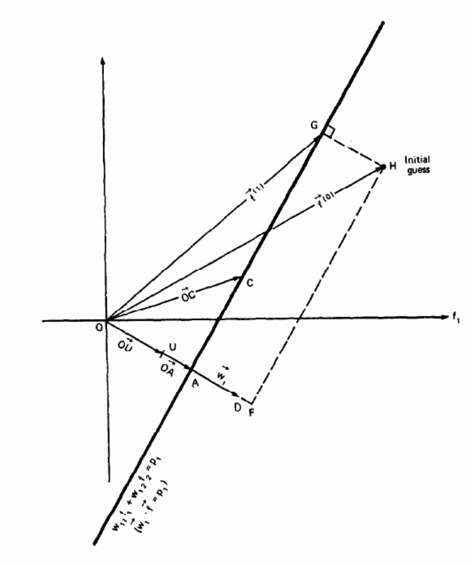

Projection onto S_i

Projection to an affine space

Projection onto $\mathcal{S}_j$

$$\mathbf{g}^* = \mathcal{P}_{\mathcal{S}_j}(\mathbf{h}) = \arg\min_{\mathbf{g}\in\mathcal{S}_j} \|\mathbf{g} - \mathbf{h}\|$$

Moving in the normal direction (minimum change) until hitting $\mathcal{S}_j$

$$\mathbf{g}^* = \mathbf{h} - \lambda \mathbf{w}_j$$
$$p_j = \langle \mathbf{w}_j, \mathbf{g}^* \rangle$$

Solution

$$\lambda = \frac{(\langle \mathbf{w}_j, \mathbf{h}\rangle - p_j)}{\langle \mathbf{w}_j, \mathbf{w}_j \rangle} \qquad \text{normalized residual}$$
$$\mathbf{g}^* = \mathbf{h} - \frac{(\langle \mathbf{w}_j, \mathbf{h}\rangle - p_j)}{\langle \mathbf{w}_j, \mathbf{w}_j \rangle}\mathbf{w}_j$$

Projection method

the algorithm

- Initial solution $\boldsymbol{\mu}^{(0)}$ (e.g. random)
- Project sequentially to constraints $1, 2, \ldots, N, 1, 2, \ldots$

$$\boldsymbol{\mu}^{(1)} = \mathcal{P}_{\mathcal{S}_1}\boldsymbol{\mu}^{(0)}$$
$$\boldsymbol{\mu}^{(2)} = \mathcal{P}_{\mathcal{S}_2}\boldsymbol{\mu}^{(1)}$$
$$\boldsymbol{\mu}^{(3)} = \mathcal{P}_{\mathcal{S}_3}\boldsymbol{\mu}^{(3)}$$
$$\ldots$$

- Repeat until convergence

Interpretation of the update

$$\boldsymbol{\mu}^{(k+1)} = \boldsymbol{\mu}^{(k)} - \underbrace{\frac{\langle \mathbf{w}_j, \boldsymbol{\mu}^{(k)} \rangle - p_j}{\langle \mathbf{w}_j, \mathbf{w}_j \rangle}}_{\tilde{p}_j} \mathbf{w}_j$$

$$p_j = \sum_{i=1}^{M} w_{ij} \mu_i = \langle \mathbf{w}_j, \boldsymbol{\mu} \rangle$$

Projection $\hat{p}_j = \langle \mathbf{w}_j, \boldsymbol{\mu}^{(k)} \rangle$ along ray j
Backprojection of the correction $\tilde{p}_j$ along ray j

Projection

$N = 2$

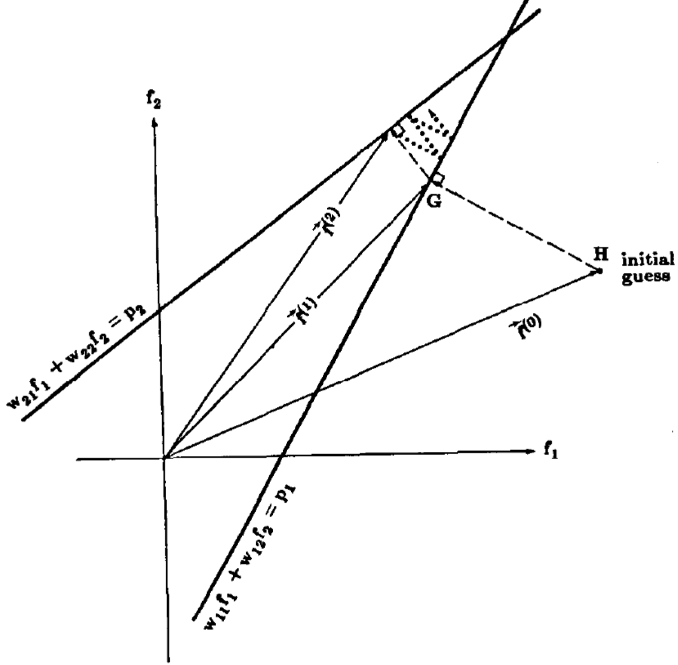

Projection method

properties

- Computationally cheap: one projection cost $O(M)$, applying all constraints $O(MN)$
- Low-memory complexity: $O(M)$ if $\mathbf{w}_{ij}$ can be calculated on the fly.
- If a solution exists, the projection method converges to it.
- Convergence may be slow.
- If no solution exists, the method may oscillate.

Projection method improvements

- Constraint ordering

Projection method improvements

- Constraint ordering
- Under/overrelaxation,

$$\boldsymbol{\mu} = \boldsymbol{\mu}^{(0)} - \alpha \frac{\langle \mathbf{w}_j, \boldsymbol{\mu} \rangle - p_j}{\langle \mathbf{w}_j, \mathbf{w}_j \rangle} \mathbf{w}_j$$

$$0 < \alpha < 2$$

Projection method improvements

- Constraint ordering
- Under/overrelaxation,

$$\boldsymbol{\mu} = \boldsymbol{\mu}^{(0)} - \alpha \frac{\langle \mathbf{w}_j, \boldsymbol{\mu} \rangle - p_j}{\langle \mathbf{w}_j, \mathbf{w}_j \rangle} \mathbf{w}_j$$

$$0 < \alpha < 2$$

- Incorporating constraints — positivity ($\mu_i \geq 0$), zero outside,...

Simplified update rules

- Binary additive case ($w_{ij} \in \{0, 1\}$)

$$\forall j,\ g_k^* = h_k - \frac{\sum\limits_{i, w_{ij}=1} h_i - p_j}{N_j}, \qquad \text{for } w_{kj} = 1,\ N_j = \sum_i w_{ij} = 1$$

- Binary multiplicative case ($w_{ij} \in \{0, 1\}$)

$$\forall j,\ g_k^* = h_k \frac{p_k}{\sum\limits_{i, w_{ij}=1} h_i}, \qquad \text{for } w_{kj} = 1$$

Projections by integration

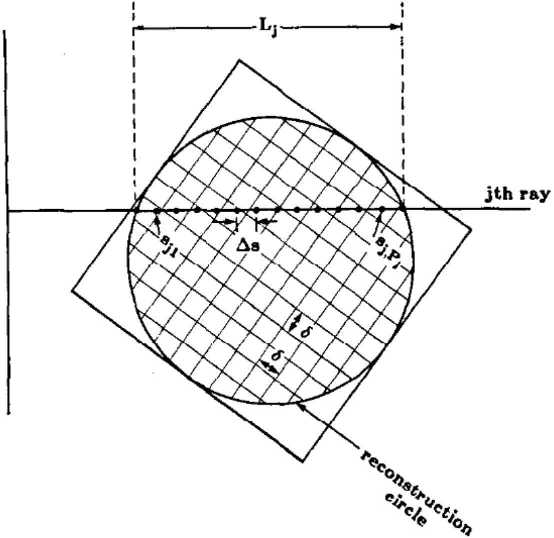

Projections by integration

$$p_j = \int \mu(r_j \cos\varphi_j - t\sin\varphi, r_j \sin\varphi_j + t\cos\varphi)\mathrm{d}t$$

$$p_j = \sum_{i=1}^{M} w_{ij}\mu_i = \langle \mathbf{w}_j, \boldsymbol{\mu} \rangle$$

$$\mu(\mathbf{x}) = \sum_{i=1}^{M} \mu_i \psi_i(\mathbf{x})$$

$$w_{ij} = \int \psi_i(r_j \cos\varphi_j - t\sin\varphi, r_j \sin\varphi_j + t\cos\varphi)\mathrm{d}t$$

$$p_j = \Delta s \sum_k \mu(r_j \cos\varphi_j - t\sin\varphi, r_j \sin\varphi_j + t\cos\varphi),$$

$$\text{with } t = \Delta s\, k$$

Backprojections by integration

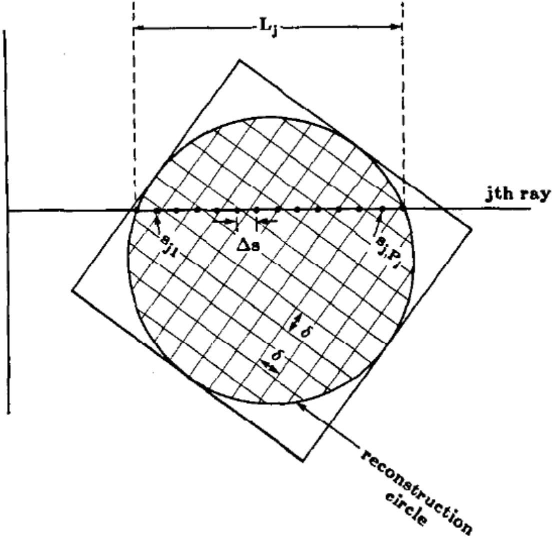

Other iterative methods

- simultaneous iterative reconstruction (SIRT), Cimmino's method — block update
- simultaneous algebraic reconstruction technique (SART) — bilinear ψ, projection by integration, Hamming window over rays
- iterative least-squares technique (ILST)
- multiplicative algebraic reconstruction technique (MART)
- iterative sparse asymptotic minimum variance (SAMV)
- (preconditioned) conjugated gradients (CG) — with regularization for ill-posed problems
- ...

Example

moving heart

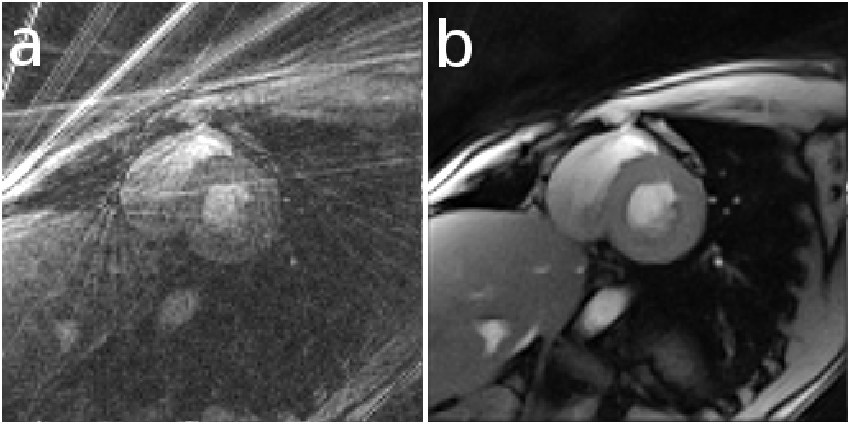

filtered back projection iterative (nonlinear)

Courtesy of Biomedizinische NMR Forschungs GmbH

Analytical methods

Algebraic reconstruction

3D CT

Radiation dose

3D computed tomography

- Technical challenges: power, cooling
- Rotation method (slice by slice)
- Spiral/helix method

Spiral method

- Acceleration: 10 min $\rightarrow$ 1 min

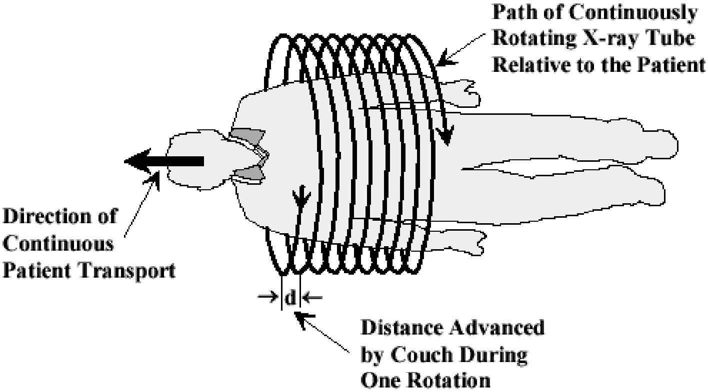

Spiral method

- Acceleration: 10 min $\rightarrow$ 1 min
- *Pitch*:

$$P = \Delta l / d$$

Δl bed shift per rotation, d slice thickness.
Normally $0 < P < 2$. Overlap for $P < 1$. Typically $P = 1.5$.

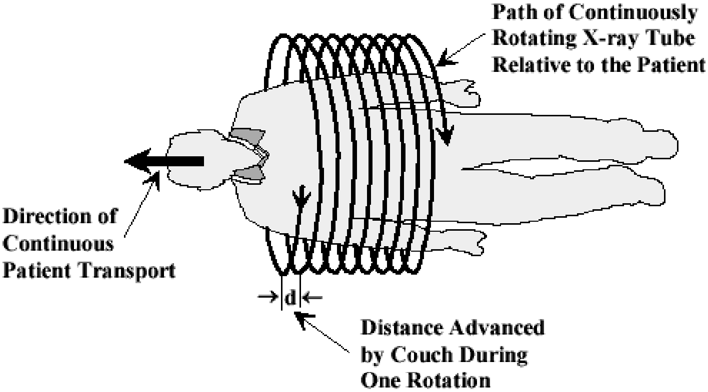

Spiral method (2)

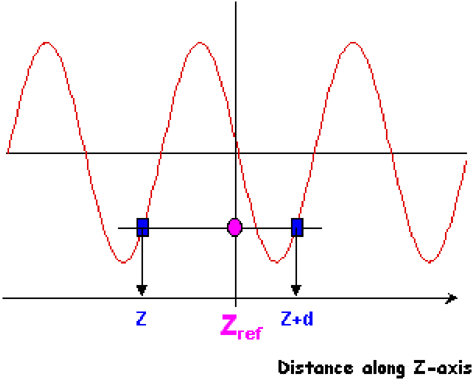

- Interpolation in z axis
- Interpolation *wide* — 1 turn. Less noise, larger effective slice thickness.
- Interpolation *Slim* — $1/2$ turn, symmetry. More noise, smaller effective slice thickness.

Spiral method (2)

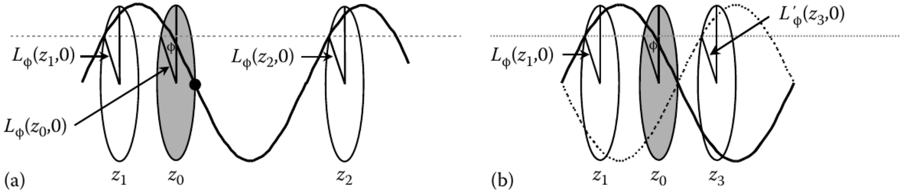

- Interpolation in z axis
- Interpolation *wide* — 1 turn. Less noise, larger effective slice thickness.
- Interpolation *Slim* — $1/2$ turn, symmetry. More noise, smaller effective slice thickness.

Multislice acquisition

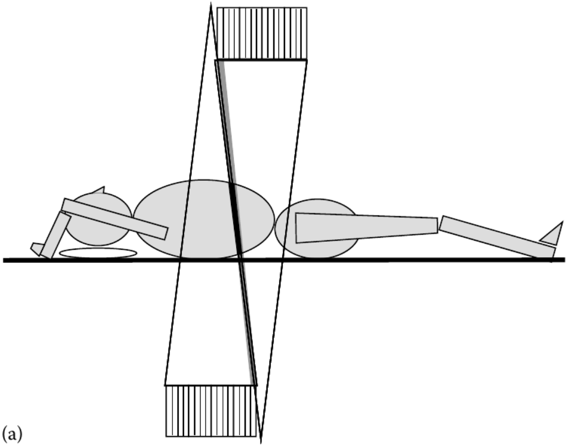

(a)

- Acceleration

Multislice acquisition

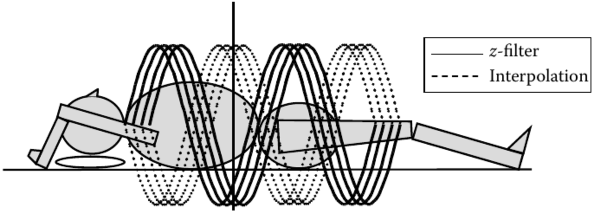

- Multi-plane reconstruction / multi-slice linear interpolation / multi-slice filtered interpolation

Multislice acquisition

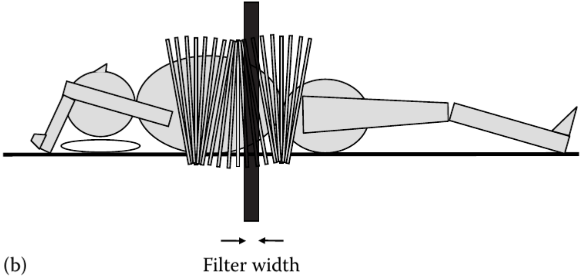

(b)

- Multi-plane reconstruction / multi-slice linear interpolation / multi-slice filtered interpolation

CT image quality

- Parameters:
  - Resolution (0.5 mm)
  - Contrast (δH, about $5 - 10$ HU.)
  - Detection threshold (about 1 mm at $\Delta H = 200$, 5 mm at $\Delta H = 5$).
  - Noise (SNR)
- Artifacts
  - Scanner defects, malfunctions, operator error
  - Metal parts (shadows)
  - Motion artifacts
  - Partial volume

Artifact examples

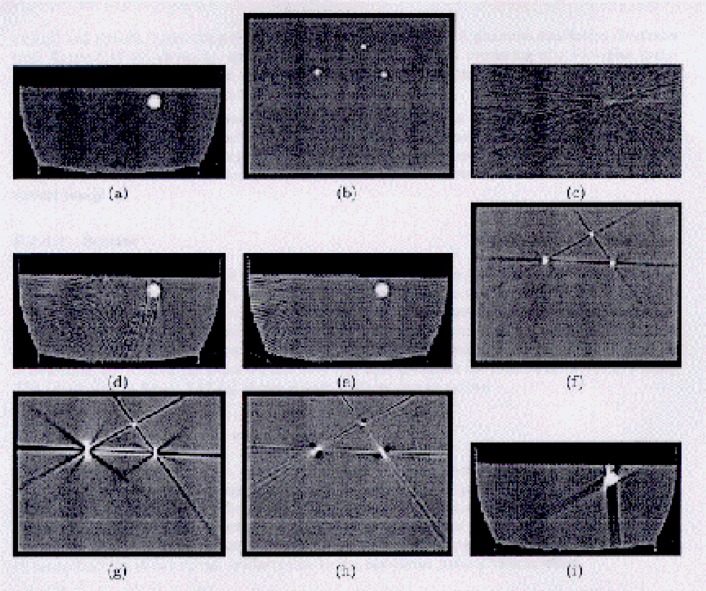

Analytical methods

Algebraic reconstruction

3D CT

Radiation dose

Radiation dose

- Absorbed dose D in units 1 Gy (gray) $= 1\,\mathrm{J/kg}$.
  Before 1 Gy = 100 rad
- Effective dose equivalent (dávkový ekvivalent) H_E [Sv] (sievert)

$$H_\mathrm{E} = \sum_i w_i H_i = \sum_i w_i c_i D_i$$

  $H = cD$. Quality factor c is 1 for X-rays and γ rays, 10 for neutrons, 20 for α particles.

  Coefficient w is organ dependent: male/female glands 0.2, lungs 0.12, breast 0.1, stomach 0.12, thyroid gland 0.05, skin 0.01. $\sum w_i = 1$.
  Before 1 Sv = 100 rem

Radiation dose

- Absorbed dose D in units 1 Gy (gray) $= 1\,\mathrm{J/kg}$.
  Before 1 Gy $=$ 100 rad
- Effective dose equivalent (dávkový ekvivalent) H_E [Sv] (sievert)

  $$H_\mathrm{E} = \sum_i w_i H_i = \sum_i w_i c_i D_i$$

  $H = cD$. Quality factor c is 1 for X-rays and γ rays, 10 for neutrons, 20 for α particles.

  Coefficient w is organ dependent: male/female glands 0.2, lungs 0.12, breast 0.1, stomach 0.12, thyroid gland 0.05, skin 0.01. $\sum w_i = 1$.
  Before 1 Sv $=$ 100 rem
- Sum the doses

Radiation dose

- Medical limit (USA) is 50 mSv/year
  (limit for a person working with radiation),
  corresponding to 1000 chest X-rays,
  or 15 head CTs,
  or 5 whole body CTs (1 CT $\approx 10\,\mathrm{mSv}$).
- low-dose CT $\approx 2 \sim 5\,\mathrm{mSv}$, PET $\approx 25\,\mathrm{mSv}$
- In radioactive background about 3 mSv/year (mainly radon).
  In Colorado (altitude $1500 \sim 4000\,\mathrm{m}$) about 4.5 mSv/year. Mean dose from medical imaging 0.3 mSv/year,
  about 3 long flights.
- aircrew members have the largest average annual effective dose about 3 mSv of all US radiation-exposed workers.
  Reason: galactic cosmic radiation, which is always present, and
  solar particle events, called "solar flares"

Radiation dose

- Medical limit (USA) is 50 mSv/year
  (limit for a person working with radiation),
  corresponding to 1000 chest X-rays,
  or 15 head CTs,
  or 5 whole body CTs (1 CT$\approx$ 10 mSv).
- low-dose CT$\approx 2 \sim 5$ mSv, PET$\approx$ 25 mSv
- In radioactive background about 3 mSv/year (mainly radon).
  In Colorado (altitude $1500 \sim 4000$ m) about 4.5 mSv/year. Mean dose from medical imaging 0.3 mSv/year,
  about 3 long flights.
- aircrew members have the largest average annual effective dose about 3 mSv of all US radiation-exposed workers.
  Reason: galactic cosmic radiation, which is always present, and
  solar particle events, called "solar flares"
- cancer related death 20 %. 1 CT=10 mSv — relative increase by $10^{-3} \sim 10^{-4}$

Computed Tomography, conclusions

- Excellent spatial resolution
- 3D image
- Fast acquisition
- Weak soft tissue contrast (contrast agents available)
- Reconstruction algorithm
- Radiation dose